Erratum: ambipolar diffusion and the molecular abundances in pre-stellar cores

Priestley, F.D.; Wurster, J.; Viti, S.

Erratum: Ambipolar diffusion and the molecular abundances in pre-stellar cores

by Felix D. Priestley,[1]★ James Wurster [2] and Serena Viti[3]

[1]*School of Physics and Astronomy, Cardiff University, Queen's Buildings, The Parade, Cardiff CF24 3AA, UK*
[2]*SUPA, School of Physics and Astronomy, University of St. Andrews, North Haugh, St Andrews, Fife KY16 9SS, UK*
[3]*Leiden Observatory, Leiden University, PO Box 9513, 2300 RA Leiden, The Netherlands*

Key words: errata, addenda – astrochemistry – MHD – stars: formation – ISM: molecules.

In Priestley, Wurster & Viti (2019), we post-processed non-ideal magnetohydrodynamic (MHD) smoothed-particle models of the collapse of sub- and super-critical prestellar cores with a time-dependent chemical network, and investigated the potential of using molecular abundances as signatures of the mode of collapse. We have since discovered that the MHD models were inadvertently run using a globally, rather than locally, isothermal equation of state. The model setup consists of a sphere of dense gas (the prestellar core) surrounded by a lower-density ambient medium, which should have a correspondingly higher temperature to ensure pressure balance. The error results in all particles having a temperature of $10\,\mathrm{K}$; the core is thus initially overpressurised, and undergoes a period of expansion before collapsing under self-gravity. As the chemical evolution of the core is highly sensitive to the history of the gas particles, the resulting molecular abundances are altered in a non-trivial manner.

We have rerun the MHD and chemical models with the correct equation of state. Figs 1 and 2 show the resulting hydrogen nuclei density n_H and CO abundance profiles for the low-density models in the midplane ($z = 0$, with the initial magnetic field in the z direction). As in the original models, while the density profiles are very similar (and effectively indistinguishable from an observational point of view), CO is significantly more depleted in the subcritical case due to more time for freeze-out of molecules on to dust grains to occur. The directly-observable quantity, the ratio of CO and hydrogen column densities (Fig. 3), shows much less variation when viewed face-on between sub- and super-critical models, again as in the original paper. The abundance profile seen edge-on for the subcritical model does differ, but the observational significance of this is limited due to the extremely low density at large distances above the midplane.

Figs 4, 5 and 6 show the integrated C_2H abundance in the high-density models, and the integrated N_2H^+ abundances for the low- and high-density models respectively, as presented in Priestley et al. (2019). In all cases, the profiles differ strongly from the original results, with sub- and super-critical models appearing much more similar when viewed along the same axis. Moreover, the significant differences caused by a change in the temperature of the background material makes any attempt to use these quantities as probes of the criticality of prestellar cores suspect.

Table 1 lists the corrected total molecular abundances of the four model prestellar cores. The values differ from those originally presented, but still remain broadly compatible with the observed
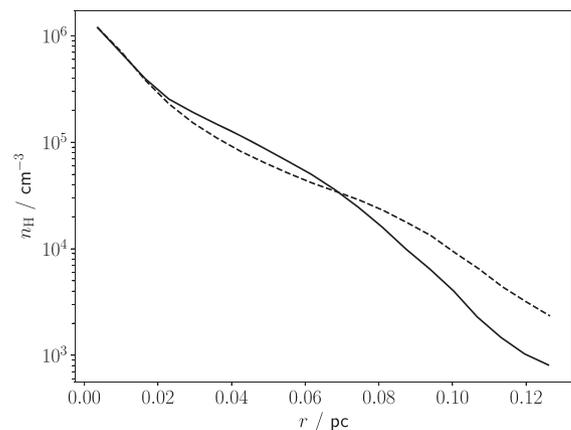
Figure 1. Hydrogen nuclei density n_H in the midplane versus radius for the LOW-SUP (solid line) and LOW-SUB (dashed line) models at the end of the simulations.
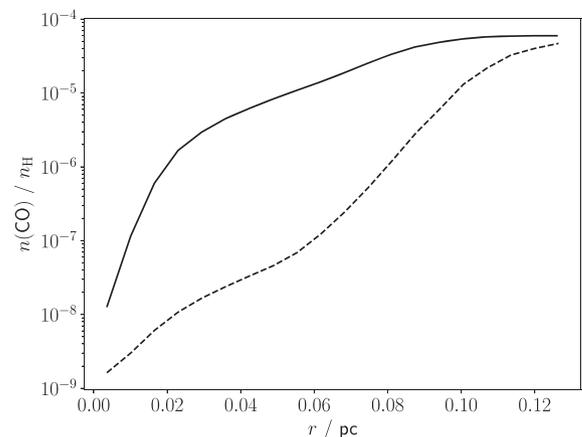
Figure 2. CO abundance in the midplane versus radius for the LOW-SUP (solid line) and LOW-SUB (dashed line) models at the end of the simulations.

values collated in Priestley et al. (2019), with the exception of CO, which now for all models has an abundance $<10^{-5}$. With the exception of L1544, which Jørgensen, Schöier & van Dishoeck (2004) find to have a CO abundance of 5×10^{-6}, other prestellar cores typically have significantly higher CO abundances. We originally
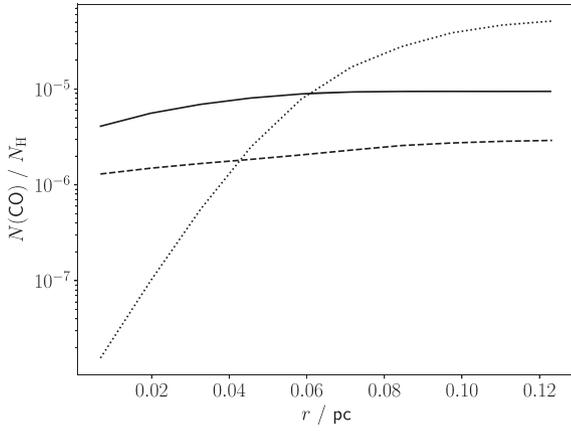
Figure 3. Integrated CO abundance versus radius for the LOW-SUP (solid line) model and the LOW-SUB model as seen from the direction of the z-axis (dashed line) and edge on (dotted line) at the end of the simulations.
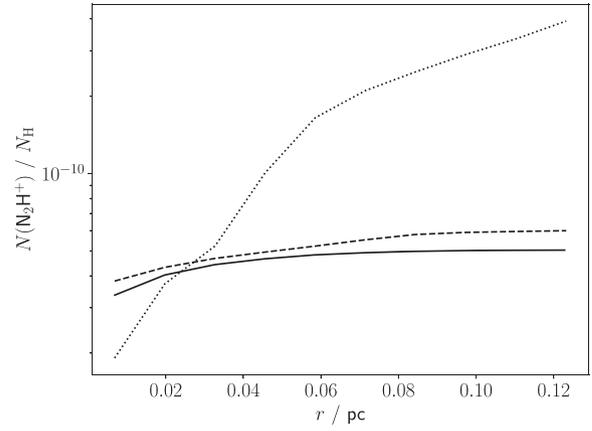
Figure 4. Integrated C_2H abundance versus radius for the HIGH-SUP (solid line) model and the HIGH-SUB model as seen from the direction of the z-axis (dashed line) and edge on (dotted line) at the end of the simulations.
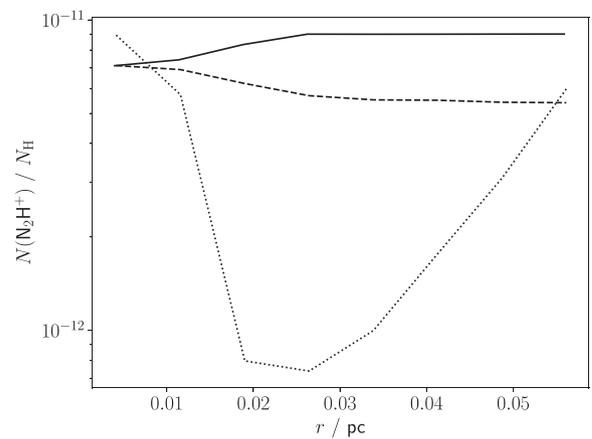
suggested that our higher-density models ($n_0 = 10^5 \, \text{cm}^{-3}$), which also produced $n(\text{CO})/n_\text{H} < 10^{-5}$, thus represented unrealistic initial conditions for prestellar cores. It now appears that even our lower-density ($10^4 \, \text{cm}^{-3}$) models may have too high an initial density to reproduce observed values.

In Priestley et al. (2019), we also presented line intensity profiles based on RADEX (van der Tak et al. 2007) calculations and the large velocity gradient approximation. Subsequent work (Yin, Priestley & Wurster, subm.), using full radiative transfer modelling, has shown that this approximation is inappropriate; for most observationally-relevant lines, optical depth effects and self-absorption are significant. We thus do not reproduce those figures here, as even with the correct underlying MHD/chemical model the results are likely to be inaccurate.

While most of the quantitative results from Priestley et al. (2019) are not supported by the new data, we consider the broader conclusions to be valid. The corrected models still show that sub- and super-critical cores can appear almost identical in terms of column density and integrated abundances (the directly observable quantities), despite molecular abundance differences of several orders of magnitude in the central regions, where the protostellar (and any protoplanetary) system will eventually form. While the proposed use

Figure 5. Integrated N_2H^+ abundance versus radius for the LOW-SUP (solid line) model and the LOW-SUB model as seen from the direction of the z-axis (dashed line) and edge on (dotted line) at the end of the simulations.

Figure 6. Integrated N_2H^+ abundance versus radius for the HIGH-SUP (solid line) model and the HIGH-SUB model as seen from the direction of the z-axis (dashed line) and edge on (dotted line) at the end of the simulations.

Table 1. Total molecular abundances, given as $a(b)$ representing $a \times 10^b$.

Molecule	LOW-SUP	LOW-SUB	HIGH-SUP	HIGH-SUB
CO	8.9(-6)	2.4(-6)	1.7(-6)	6.8(-6)
CS	2.5(-8)	1.7(-9)	2.3(-8)	1.4(-7)
CN	5.8(-10)	6.6(-10)	8.1(-10)	2.1(-9)
NH_3	1.7(-8)	1.4(-8)	3.3(-8)	3.3(-7)
HCN	8.9(-10)	3.2(-10)	1.7(-8)	1.1(-7)
C_2H	7.1(-11)	1.6(-10)	4.0(-11)	8.7(-11)
C_3H_2	1.0(-9)	5.0(-10)	1.6(-10)	3.4(-10)
N_2H^+	4.8(-11)	5.5(-11)	8.8(-12)	5.7(-12)
CH_3OH	2.9(-10)	1.6(-10)	6.5(-10)	1.7(-8)
H_2CO	5.0(-9)	6.8(-10)	3.5(-9)	4.7(-9)
HCO^+	3.1(-9)	1.3(-9)	4.1(-10)	2.5(-10)
HC_3N	3.0(-10)	4.2(-12)	9.5(-10)	4.1(-9)

of N_2H^+ abundance profiles as a tracer of magnetic criticality, for example, does not now hold up (Figs 5 and 6), the fact that the degree of magnetic support strongly influences the chemical evolution of prestellar cores, yet produces few (if any) observational signatures of this, remains worth noting.

ACKNOWLEDGEMENTS

DATA AVAILABILITY

The data underlying this paper will be made available upon request.

REFERENCES

Jørgensen J. K., Schöier F. L., van Dishoeck E. F., 2004, A&A, 416, 603
Priestley F. D., Wurster J., Viti S., 2019, MNRAS, 488, 2357
van der Tak F. F. S., Black J. H., Schöier F. L., Jansen D. J., van Dishoeck E. F., 2007, A&A, 468, 627

This paper has been typeset from a TEX/LATEX file prepared by the author.